

## **Analysis of the Necking Behaviors with the Crystal Plasticity Model using 3-Dimensional Shaped Grains**

Jong-Bong Kim<sup>1, a</sup> and Jeong Whan Yoon<sup>2, b</sup>

<sup>1</sup>Dept. of Automotive Engineering, Seoul Nat. Univ. Sci. Technol., 172, Gongneung-2 Dong, Nowon-Gu, Seoul, Korea

<sup>2</sup>Faculty of Engineering & Industrial Sci., Swinburne Univ. of Technol., PO Box 218, Hawthorn, Victoria, 3122, Australia

<sup>a</sup>jbkim@seoultech.ac.kr, <sup>b</sup>jyoon@swin.edu.au

**Keywords:** Necking, Crystal Plasticity, Grains, Texture.

**Abstract.** Without initial imperfection and damage evolution model, it is difficult to analyze the necking behavior by finite element analysis with continuum theory. Moreover, the results are greatly dependent on the size of the initial imperfection. In order to predict necking phenomenon without geometric imperfection, in this study, a crystal plasticity model was introduced in the 3-dimensional finite element analysis of tensile test. Grains were modeled by an octahedron and different orientations were allocated to each grain. Damage model was also used to predict the sudden drop of load carrying capacity after necking and to reflect the void nucleation and growth on the severely deformed region. Well-known Cockcroft-Latham damage model was used. Void nucleation, growth and coalescence behavior during necking were predicted reasonably.

### **Introduction**

In sheet metal forming processes, necking and fractures need to be accurately predicted in order to make defect free products. A forming limit diagram (FLD) [1-3] is a well-known measure for fracture prediction in the ordinary stamping process. In specific sheet metal forming processes such as the incremental forming process, however, local fracture strain is important because the deformation takes place in very local regions. This local deformation is considered to be the main reason of the formability improvement in incremental sheet metal forming.

In order to investigate the fracture behavior after necking, tensile test was subjected to the finite element analysis based on the crystal plasticity and damage evolution. It is assumed that voids or cracks are nucleated where stress is concentrated by orientation mismatch. Each grain has its own orientation. Therefore, the orientation of one grain does not coincide with that of its neighbor grains and stress concentration may take place. To analyze the stress concentration inside a grain, crystal plasticity model was introduced in the analysis of the tensile test. The crystal plasticity model is widely used to predict material behaviors such as anisotropy development, twinning, and crack initiation. Yoon et al. [4] studied the anisotropic hardening behavior of cube textured aluminum alloy sheets using the crystal plasticity. Choi et al. [5] analyzed the stress concentration on the grain boundary and the twinning behavior of Mg alloys. Dao and Li [6] predicted crack initiation in bending using the crystal plasticity model. They used the representative volume element (RVE) method to assign the orientation to regular elements.

Kim et al. [7, 8] predicted the necking behavior of aluminum 6022-T4 by the crystal plasticity finite element method. They analyzed the necking initiation successfully without any geometrical imperfections. They carried out the 3-dimensional analysis using 2-dimensional shaped grains. It means that the grain is modeled by hexagonal column by extruding hexagon in thickness direction. In the analysis, they found that the necking can be predicted without any geometrical imperfections by crystal finite element analysis. However, they could not consider the orientation mismatch along thickness direction.

To consider the orientation mismatch along the thickness direction, the analysis was carried out using 3-dimensional shaped grains in this study. Each grain is modeled by an octahedron and discretized by many tetrahedron elements. By incorporating damage evolution model, void nucleation, growth and coalescence behavior were analyzed.

### Theory

The crystal plasticity model accounts for the deformation of a material by crystallographic slip and for the reorientation of the crystal lattice. In this work, a rate-dependent TBH model, which was well described by Dao and Asaro [9], was employed. The detailed implementation procedures were described in the work of Yoon et al. [4] and Kim et al. [7, 8].

Wierzbicki et al. [10] intensively reviewed the prediction capability of crack for various damage models. Among many models, Cockcroft-Latham damage model was used in this study. Cockcroft and Latham [11] described the damage as a function of principal stress and effective strain. In this study, their model was modified as follows.

$$dD = \begin{cases} \frac{\sigma_1 d\epsilon_1}{\sigma_{cr} \cdot \Delta\epsilon_{cr}} & \text{for } \sigma_1 \geq \sigma_{cr} \text{ and } d\epsilon_1 \geq 0, \\ 0 & \text{for } \sigma_1 < \sigma_{cr} \text{ or } d\epsilon_1 < 0 \end{cases} \quad (1)$$

$$D = \int dD \quad (2)$$

In Eq. (1),  $\sigma_{cr}$  is the critical major stress over which damage starts to accumulate and  $\Delta\epsilon_{cr}$  is the plastic strain amount from damage initiation to fracture. In this study,  $\Delta\epsilon_{cr}$  is called the “degradation plastic strain”. If the major stress is less than the critical stress, or if the deformation along the major stress is compressive, the damage increment is zero.  $\sigma_{cr}$  and  $\Delta\epsilon_{cr}$  are material parameters that should be determined. Based on the works of Kim et al. [7, 8], 500 MPa and 0.05 were used as the value of  $\sigma_{cr}$  and  $\Delta\epsilon_{cr}$ , respectively.

### Model Description and Material Properties

To predict necking in tensile tests, a 6022-T4 aluminum alloy sheet was subjected to the finite element analysis based on the crystal plasticity model. The crystal plasticity model was implemented into the finite element code ABAQUS/Explicit [12] via a user-defined material subroutine (VUMAT). For the computational effectiveness, analysis of tensile test was carried out for only a part of a tensile specimen as shown in Fig. 1. Considering the plane symmetry, the top surface of the analysis domain was treated as a symmetric boundary condition. Tensile displacements,  $U_x$  and  $-U_y$ , were imposed on the right and left surface. Displacement boundary condition for the nodes on the bottom surface was calculated to guarantee the volume conservation during plastic deformation of isotropic materials, i.e.,

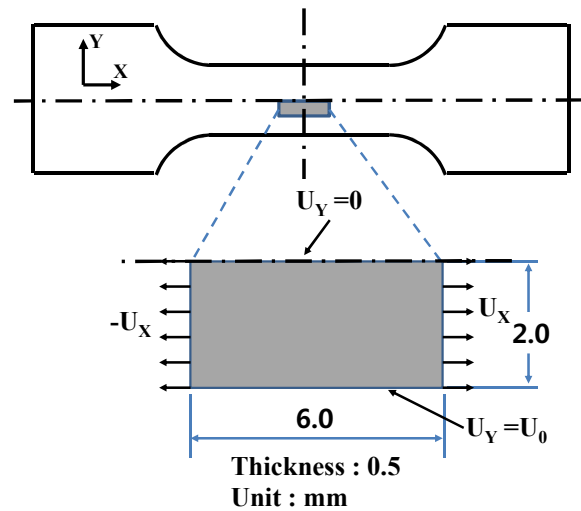


Fig. 1 Definition of analysis domain and boundary conditions for tensile test

$$\varepsilon_y = -0.5\varepsilon_x \quad (3)$$

$$\ln \frac{2.0+U_0}{2} = -0.5 \ln \frac{3.0+U_x}{3} \quad (4)$$

Fig. 2 shows the analysis model and grain shape. Grain shape is assumed to be a regular octahedron as shown in Fig. 2(c). Considering the shape change during rolling process, grain size is assumed to be about 0.2, 0.1, and 0.05 mm in x, y, and z direction, respectively. Each grain is discretized by many elements and the same orientation angles are allocated to all elements in each grain as shown in Fig. 3(a). The elements in each grain are sorted in one group and the same orientations are allocated. Fig. 3 shows the contour of ‘ $-\cos(\phi)$ ’, where  $\phi$  is the second Euler angle. It is shown that the same orientation angles are allocated to all elements in each grain. Fig. 3(b) shows the (111) pole figure of materials.

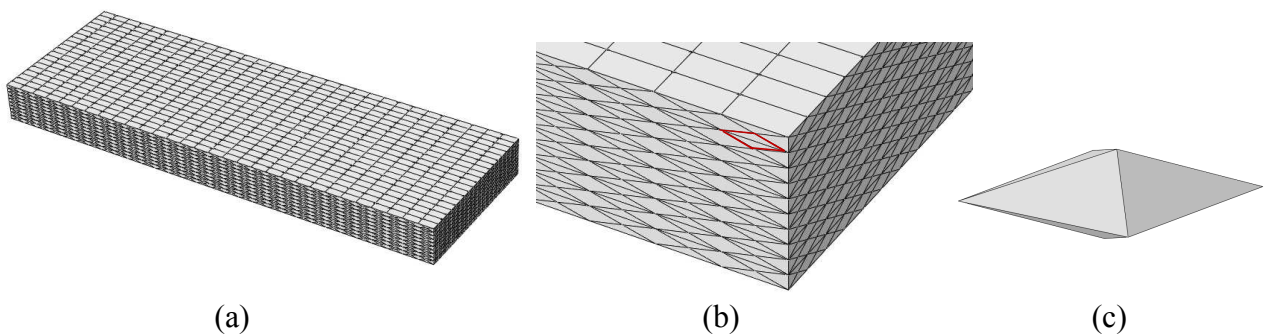


Fig. 2 Division of specimen by octagon grains: (a) full model, (b) magnified view and (c) octahedron shape of grain

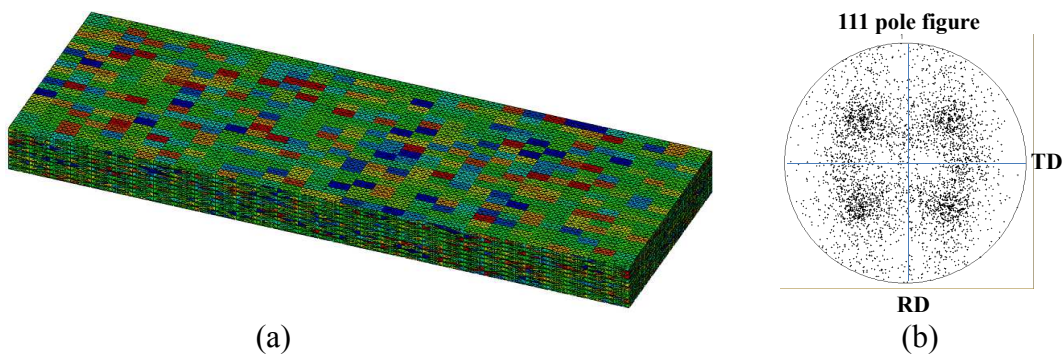


Fig. 3 (a) Contour of “ $-\cos(\phi)$ ” showing the correct allocation of orientation angles and (b) (111) pole figure for 6022-T4 aluminum sheet sample.

A 6022-T4 aluminum alloy sheet was used in the analysis. Basic mechanical properties were obtained by tensile test along the rolling direction. The uniform and total elongations are 21.5% and 26.6%, respectively. The stress-strain relation is described as

$$\sigma = 469.7(\varepsilon + 0.002)^{0.255} \text{ (MPa)} \quad (5)$$

where,  $\sigma$  is plastic flow stress and  $\varepsilon$  is effective plastic strain. The slip resistance of all slip systems at one material point is taken to be the same. The slip system hardening is assumed to follow the macroscopic hardening behavior. Through several trial analyses, the average Taylor factor was determined to be 2.512 and the following hardening equation was used for the slip system hardening.

$$\sigma = 187.0(\varepsilon + 0.002)^{0.255} \text{ (MPa)} \quad (6)$$

## Results and Discussions

Fig. 4 shows the effective stress distributions at several time stages. In Figs 4 and 5,  $\epsilon_g$  is the gage strain calculated from the initial length and tensile displacement. As expected, stress concentration takes place at many points. This stress concentration is considered to be caused by orientation mismatches between neighbor grains. As tensile strain increases, the stress concentration also becomes bigger until the stress reaches the critical value. If the major stress becomes greater than this critical value, damage starts to accumulate and stress is lowered by softening (see Figs. 4(c) and (d)). With this reason, the stress on the necking area is lower than the stress on the other area.

Fig. 5 shows the damage evolution. When the gage strain is 0.014, there is no damaged element. When the gage strain is 0.042, many damaged elements are shown in wide area. This is similar to void nucleation. As tensile strain increases more, damaged area increases and finally neighboring damaged regions get together. These are correlated to the void growth and void coalescence phenomena. Finally, most of elements in necking region were damaged. In the analysis, necking starts to take place when gage strain is about 0.17. This is lower than 0.215 which is obtained in the experiment. This is because 500 MPa of  $\sigma_{cr}$  in Eq. 1 is too low. For the accurate prediction of uniform elongation, the value of  $\sigma_{cr}$  have to be determined accurately by several analyses.

In this study, prediction capability of necking using crystal plasticity model was investigated. It is shown that the necking behavior and direction can be successfully predicted.

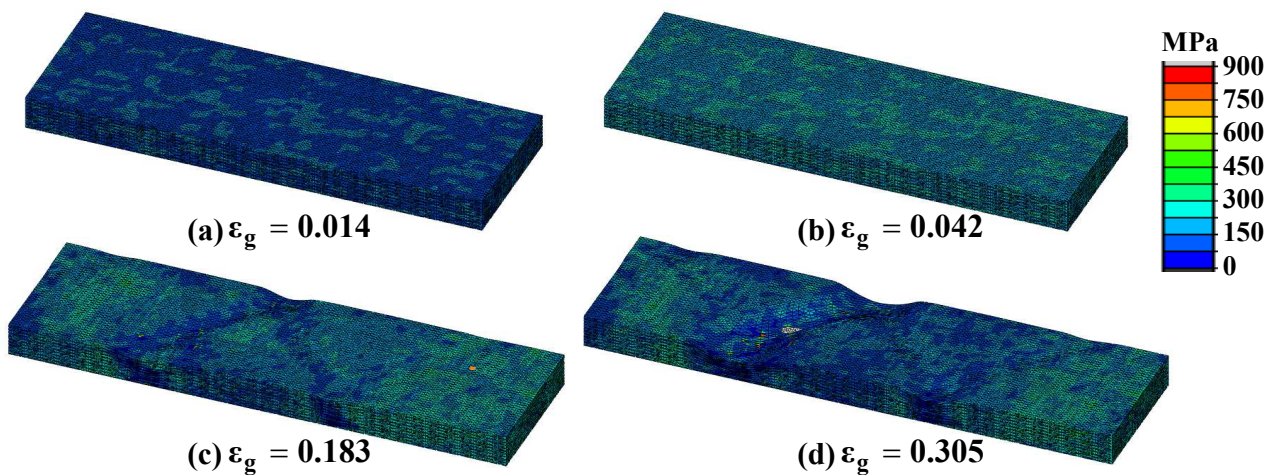


Fig. 4 Effective stress distribution.

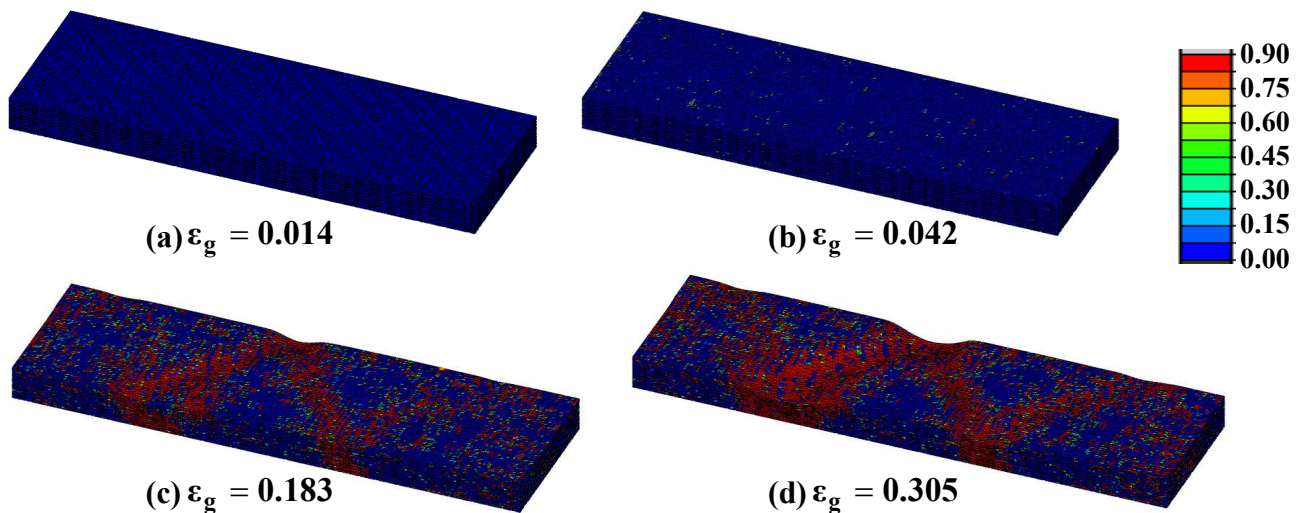


Fig. 5 Damage distribution.

## Summary

The necking behavior of 6022-T4 aluminum sheet was analyzed based on the crystal plasticity model. Tensile specimen was modeled by octahedron shaped 3-dimensional grains. Each grain was discretized by many elements and the same orientations were allocated to all elements in the same grain. To describe the sudden drop of load carrying capacity after necking, a damage model was employed. Stress concentration was observed at many points due to the orientation mismatch at several points. This stress concentration was considered to cause damage initiation and evolution. The void nucleation, growth and coalescence phenomena were well described by the proposed methodology. As a results, the necking behavior of aluminum 6022-T4 alloy sheets was successfully predicted with octahedron shaped grain without any initial geometric imperfections.

## Acknowledgements

This work was supported by a National Research Foundation of Korea Grant funded by the Korean Government (NRF-2011-013-D00001).

## References

- [1] S.B. Kim, H. Huh, H.H. Bok and M.B. Moon: J. of Mater. Process. Technol., Vol. 211 (2010), p. 851-862.
- [2] M. Kuroda and V. Tvergaard: Int. J. of Solids and Struct., Vol. 37 (2000), p. 5037-5059.
- [3] T.B. Stoughton and J.W. Yoon: Int. J. Plasticity, Vol. 27 (2011), p. 440-459.
- [4] J.W. Yoon, F. Barlat, J.J. Gracio and E. Rauch: Int. J. Plasticity, Vol. 21 (2005), p. 2426-2447.
- [5] S.-H. Chio, D.H. Kim, S.S. Park and B.S. You: Acta Mater., Vol. 58 (2010), p. 320-329.
- [6] M. Dao and M. Li: Philosophical Magazine A, Vol. 81 (2001), p. 1997-2020.
- [7] J.-B. Kim, W.-S. Seo, S.-H. Hong and J. W. Yoon: Steel Research International, Special Edi. (2012), p. 1187-1190.
- [8] J.-B. Kim, S.-H. Hong and J. W. Yoon: Trans. KSPE, Vol. 29 (2012), p. 818-823
- [9] M. Dao and R.J. Asaro: Mech. Mater., Vol. 23 (1996), p. 71-102.
- [10] T. Wierzbicki, Y. Bao, Y.-W. Lee and Y. Bai: Int. J. Mech. Sci., Vol. 47 (2005), p. 719-743.
- [11] M.G. Cockcroft and D.J. Latham: J. of the Institute of Metals, Vol. 96 (1968), p. 33-39.
- [12] ABAQUS Inc: *ABAQUS theory manual*, Version 6.4 (2006).